Chronic treatment with fluoxetine downregulates mitochondrial activity in parvalbumin interneurons of prefrontal cortex

Abbreviated title: Fluoxetine PFC TRAP

Elias Jetsonen[1], Ilida Suleymanova[2], Eero Castrén[1*], Juzoh Umemori[1, 3*]

1 Neuroscience Center, HiLIFE, University of Helsinki, Finland.

2 Faculty of Biological and Environmental Sciences, University of Helsinki, Finland

3 Gene and cell technology, A.I. Virtanen Institute, University of Eastern Finland

Shared Corresponding Authors:

Eero Castren, MD, PhD

Neuroscience Center, HiLIFE, University of Helsinki, Finland

Email: eero.castren@helsinki.fi

Address: University of Helsinki, P.O. Box 56, 00014 Helsinki, Finland

Juzoh Umemori, PhD

Neuroscience Center, HiLIFE, University of Helsinki, Finland

Gene and Cell Technology, A.I. Virtanen Institute, University of Eastern Finland

Email: juzoh.umemori@uef.fi

Address: A.I. Virtanen Institute, P.O. Box 1627, 70211 Kuopio, Finland

Abstract

Chronic treatment with fluoxetine, a widely prescribed selective serotonin reuptake inhibitor (SSRI), is known to promote neural plasticity. The role of fluoxetine in plasticity has been particularly tied to parvalbumin-positive interneurons (PV-INs), which are critical regulators of inhibitory tone and synaptic plasticity. Our previous studies have highlighted behavioral plasticity and gene expression changes in the visual cortex and hippocampus after chronic treatment with fluoxetine. However, the impact of fluoxetine treatment on gene expression and neuronal function in the prefrontal cortex (PFC) remains unclear. This study aimed to investigate the effects of chronic fluoxetine treatment on PV-INs in the PFC. Using Translating Ribosome Affinity Purification (TRAP), we found that fluoxetine treatment downregulated pathways involved in mitochondrial energy production, including multiple steps of the respiratory chain. Upregulated genes were associated with phosphatase activity, voltage-gated potassium channels, and amino acid transmembrane transport. Mitochondrial analysis for sorted cells demonstrated mitochondrial membrane potential was reduced in PV-INs, but increased in non-PV-INs in the PFC. These observations indicate altered mitochondrial dynamics between the cell types and reduced mitochondrial activity in PV-INs, potentially contributing to their disinhibition. Immunohistochemical analyses further demonstrated reduced PV expression and weakened perineuronal nets in specific PFC regions, suggesting elevated plasticity, and potentially explaining the modulation of fear and anxiety-related behaviors that were previously observed. Our results underscore the differential impact of chronic fluoxetine on gene expression and mitochondrial function in PV-INs, suggesting region-specific disinhibition and enhanced synaptic plasticity in the PFC.

Keywords

Parvalbumin interneurons, SSRI, neural plasticity, cell-type specific transcriptome, mitochondria, BDNF, TrkB

Introduction

Fluoxetine is a widely used antidepressant belonging to the pharmacological group of selective serotonin reuptake inhibitors (SSRI). Preclinical studies have shown that fluoxetine induces juvenile-like plasticity in the adult rodent brain and promotes synaptic plasticity and network remodeling [1–3]. These neuroplastic effects have been observed in diverse neural systems including the visual cortex [4], fear conditioning network [5], and reversal learning [6]. In addition, fluoxetine appears to restore impaired neurogenesis in the rodent hippocampus [7]. Mechanistically, antidepressants have been shown to directly bind to neurotrophic receptor tyrosine kinase (NTRK2, or TrkB) and stabilize its dimer to enhance BDNF signaling through TrkB [8].

Parvalbumin positive interneurons (PV-INs), one of the largest populations of GABAergic interneurons that synchronize local circuit neural activity [9], have a key role in gamma oscillations [10] and are known to control neural plasticity [11]. Specifically, TrkB-receptor activation in PV-INs is necessary and sufficient for cortical plasticity in the visual cortex, as was previously demonstrated in our studies using conditional knockout mice and optogenetics [12]. Additionally, heterozygous removal of TrkB in PV-cells blunts fluoxetine's effect on reversal learning [6]. Most PV-cells are surrounded by a specific extracellular matrix formation called the perineuronal net (PNN), which stabilizes synaptic connections and restricts neural plasticity, particularly following critical periods of development [13]. The PNN surrounds the soma and proximal dendrites of PV-INs and is composed of hyaluronan, chondroitin sulfate proteoglycans, and linking proteins [14]. PV-INs play a crucial role in maintaining the excitatory-inhibitory balance (E/I-balance) and optimizing synchronized signal processing in the cortex [15]. Notably, mature PNN reduce the E/I-balance by blocking AMPA receptor trafficking [16], inhibiting TrkB activity [17], and influencing the firing potential of PV-INs [18]. This process of increasing E/I-balance, known as disinhibition, has been observed following either administration of venlafaxine [19] or optical activation of TrkB in PV-INs [12].

Mitochondria generate the majority of cellular energy, primarily in the form of ATP, through oxidative phosphorylation—which is essential for neuronal plasticity observed in synaptic transmission and memory formation [20,21]. This process begins with the oxidation of pyruvate in the Krebs cycle, which produces NADH. NADH donates electrons to the electron transport chain, driving the pumping of protons across the inner mitochondrial membrane and creating a membrane potential, which is then utilized by ATP synthase to produce ATP [22]. A critical component of the mitochondrial import machinery is the Translocase of the Outer Membrane 22 (Tomm22), which plays a pivotal role in maintaining mitochondrial function by facilitating the import of nuclear-encoded proteins and regulating mitophagy [23,24]. Previous studies have indicated that fluoxetine can affect mitochondrial function in neurons, although the findings have been inconsistent with both upregulation and downregulation reported following acute or chronic administration [25]. For instance, a proteomic study using rat hippocampus found upregulation of proteins related to mitochondrial energy production [26]. In contrast, other studies observed that fluoxetine reduced mitochondrial respiration and ATP synthesis, particularly at high concentrations [27,28]. Additionally, Agostinho et al found that chronic fluoxetine decreased the activity of respiratory chain complex IV in the hippocampus [29]. These discrepancies likely arise from the heterogeneity of neural tissues and the diversity of cell types. However, cell-type specific analyses have not been conducted yet.

The prefrontal cortex (PFC) is a functionally diverse brain region critical for decision-making, emotional regulation, and motor planning. It has connections to multiple subcortical and cortical regions [30], including the midbrain, which modulates reward processing, motivation, and cognitive function [31], and the hippocampus and amygdala which are shaping network configurations essential for cognitive flexibility and emotional processing [32]. Within the PFC, the prelimbic area (PL) is primarily involved in emotional processing and the expression of fear, while the infralimbic area (IL) is crucial for fear extinction and emotional inhibition—both of which are essential for adaptive behavior [33,34]. The anterior cingulate area (ACA), along with the supplementary motor cortex (M2), play a central role in cognitive control, error monitoring, and motor planning,

102 supporting cognitive flexibility and motor adaptation [35]. However, the specific effects of chronic
103 fluoxetine treatment on the different PFC areas remain elusive.
104 We previously conducted a transcriptomic analysis specifically for PV-INs in the hippocampus
105 using a translating ribosome affinity purification (TRAP) following chronic treatment with fluoxetine
106 and found changes in gene expression—such as those involved in PNN construction and synaptic
107 formation[6]. In this study, we applied the TRAP to the PFC and identified an upregulation of
108 plasticity-related genes and a downregulation of mitochondria-related genes in PV-INs. We further
109 analyzed mitochondrial function in FACS-sorted PV-INs, and performed immunohistochemical
110 analysis to assess mitochondrial mass and PNN formation across specific subregions of the PFC.
111
112 **Material and Methods**
113 Mice
114 For the TRAP, transgenic mice expressing FLEX-L10a conjugating GFP specifically in PV-INs were
115 produced by mating females from a homozygous PV-specific Cre line ($PV^{cre/cre}$; Pvalb-IRES-Cre, JAX:
116 008069, Jackson laboratory)[36] with males from an homozygous mice expressing GFP-L10a [37]
117 (B6;129S4-Gt(ROSA)26Sor $^{tm9(EGFP/Rpl10a)Amc}$/J, 024750, Jackson laboratory) . For PV-INs specific
118 mitochondria analysis, mice were obtained by crossing male transgenic mice harboring double
119 inverted open reading frame (DIO)-expressing tdTomato (B6.Cg-*Gt(ROSA)26Sor*$^{tm14(CAG-tdTomato)Hze}$/J,
120 RRID:IMSR_JAX:007914, Jackson laboratory) [38] with female mice of the homozygous PV specific
121 Cre line ($PV^{cre/cre}$)[36].
122 All mice were kept in a room at 23±2°C with a 12-hr light/dark cycle (lights on at 6:00 a.m.)
123 with access to food and water ad libitum. Three months old male mice are used for this study. All
124 experiments were carried out in accordance with the European Communities Council Directive
125 86/6609/EEC and the guidelines of the Society for Neuroscience and were approved by the County
126 Administrative Board of Southern Finland (License number: ESAVI/38503/2019).
127

128 Fluoxetine treatment

129 Fluoxetine (0.008 % w/v) was administered in drinking water for 14 days in all experiments. For both
130 control and treated groups, drinking water included 0.1 % saccharine for equalizing taste of water.
131 The same treatment conditions were used for all experiments.

132

133 TRAP

134 TRAP analysis was performed according to previously published protocol [39]. Briefly, we isolated
135 prefrontal cortex (PFC) from mice expressing GFP tag in ribosomes of PV-cells, as mentioned above.
136 The isolated PFC were stored in -80 C between isolation and TRAP analysis. After lysating the PFC, the
137 GFP-tagged ribosomes were precipitated using magnetic beads coated with anti-GFP antibodies.
138 Quality of RNA was assessed by Bioanalyzer (Agilent, California, US), and one sample was excluded
139 due to low RNA integrity (2.4 while it was between 7.6-9.5) (Supplemental fig 2). Actively translated
140 mRNA co-precipitated and were sequenced using HiSeq2500 (Illumina, CA, USA) with SMART-Seq v4
141 Ultra Low Input RNA kit (Takara, Japan) for making cDNA library.

142

143 PV-INs specific assay for mitochondrial mass, membrane potential, ATPassay

144 PV-TdT mice were anesthetized using pentobarbital and transcardially perfused with cooled N-
145 methyl-D-glucamine buffer [40]to preserve cells. Brains were isolated, and hippocampus, prefrontal
146 cortex and rest of the cortex were dissected. Cells were dissociated using Neural Tissue Dissociation
147 Kit (Miltenyi, Germany) according to manufacturer's protocol. The cells were then FACS sorted to PV
148 and non-PV cells based on TdT expression. To measure mitochondrial mass, the cells were stained
149 with MitoTracker Green (Thermo Fisher, Massachusetts US) for 30 min in 37 C. To measure
150 mitochondrial membrane potential, the cells were stained with 5 nm Rhodamine 123 [41], for 30 min
151 in +4 C. The cells were centrifuged at 300 g for 10 min and diluted with D-PBS before proceeding to
152 the second round of FACS. During sorting, fluorescence was measured for each cell. Using the sorted

153 cells, ATP was detected using CellTiter (Promega, Wisconsin US) according to manufacturer's
154 protocol. Luminescence was detected with Varioskan Flash (Thermo Fisher, Massachusetts US).
155
156 Immunohistochemistry on PV, PNN and TOMM22
157 Mice were deeply anesthetized and perfused with 4 % PFA in PBS. The brains were cut into 40 µm
158 sections and stored in +4 °C until further processing. Sections were then washed with PBST and
159 blocked using bovine serum albumin and donkey serum. The sections were stained with primary
160 antibodies overnight and, after additional PBST washing, secondary antibodies for 1 h in room
161 temperature. Details of used primary and secondary antibodies and their dilutions are listed in
162 supplemental table 1. Images were obtained using Andor Dragonfly (Oxford Instruments, United
163 Kingdom).
164
165 **Imaging analysis**
166 The entire PFC was imaged obtaining multiple frames and Z-stack. Images were stitched using ImageJ
167 and the best layer of Z-stack was manually selected for analysis. Subregions were identified using a
168 reference atlas [42]. Cell borders were detected using custom scripts developed in MATLAB (The
169 MathWorks, Massachusetts, US), which employed a combination of morphological feature analysis
170 and thresholding technique. Cells were detected using PV and PNN staining, and data of overlapping
171 cells was combined. PV and TOMM22 signal intensities were measured in cells detected by PV shape
172 and PNN signal intensity was measured in cells detected by PNN shape.
173
174 Experimental design and statistical analysis
175 Statistical analysis for TRAP was conducted using R and package DESeq2 [43]. Multiple test correction
176 was performed using Benjamini-Hochberg procedure, and q-value (corrected P-value) of 0.1 was
177 considered significant. Detected differentially expressed genes (DEGs) are listed in supplemental
178 table 2. Pathway analysis was performed using package clusterProfiler [44]. Resulting pathways were

clustered and visualized using the function “emapplot_cluster”. All detected pathways are listed in supplemental table 3.

Data from immunohistochemical, mitochondrial membrane potential, mitochondrial mass, and ATP assays were analyzed by two-way ANOVA followed by post hoc test with multiple test correction using Šídák’s method, or Chi-square test when suitable. Statistical analyses were performed using Prism 9 (GraphPad Software, California, US). P-value < 0.05 was considered significant. Statistical details of these tests are listed in supplemental table 4.

188

189 **Results**

190 ***Identification of PV-IN specific gene expression changes following chronic fluoxetine***

191 ***treatment***

192 After two weeks of fluoxetine treatment, we performed Translating Ribosome Affinity Purification

193 (TRAP) analysis on parvalbumin-positive interneurons (PV-INs) (Fig. 1a-b). Following the application

194 the Benjamini-Hochberg procedure for multiple test correction, we identified 315 DEGs ($q < 0.1$) (Fig

195 1c, Supplemental table 2). The top 50 DEGs with the lowest q-values are shown in Fig 1d.

196

197

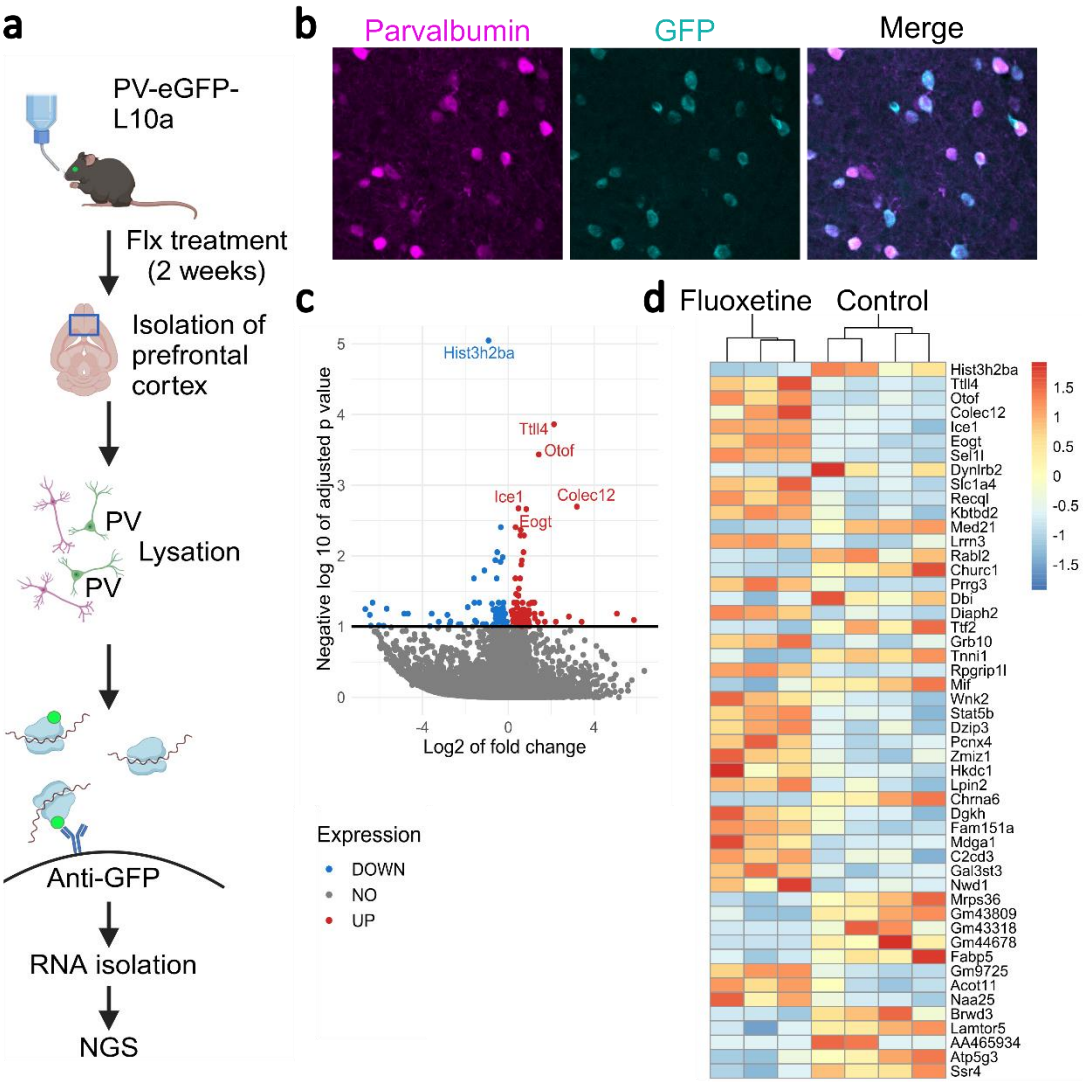

198

199 Figure 1: Fluoxetine-induced transcriptional changes in PV-INs from the PFC.

200 **a)** PV-eGFP-L10a mice were treated with fluoxetine or regular water for 2 weeks, and their PFC
201 were isolated post-euthanasia. GFP-tagged translating ribosomes binding mRNA were
202 precipitated from cell lysate using magnetic beads coated with anti-GFP antibodies, enabling the
203 isolation of ribosome-bound mRNA. The isolated mRNA was then converted into cDNA and
204 sequenced using next-generation sequencing (NGS). **b)** Representative PFC section from PV-
205 eGFP-L10a mouse stained with parvalbumin antibody. GFP co-localizes with parvalbumin,
206 confirming the specificity of the PV-IN labeling **c)** Volcano plot showing differentially expressed
207 genes in PV-INs, with the x-axis representing the magnitude of change (log2 fold change) and the
208 y-axis representing statistical significance (−log10 adjusted p-value) on. Upregulated genes are
209 highlighted in red and downregulated genes in blue, providing a visual overview of the

210 transcriptional changes induced by fluoxetine. **d)** Heatmap of 50 most differentially expressed
211 genes (DEGs) in PV-INs after chronic fluoxetine treatment, illustrating the extent and pattern of
212 gene expression changes.

213

214 We then conducted a pathway enrichment analysis using Gene Ontology (GO) Molecular Function -
215 pathways for these DEGs and identified upregulation in 30 and downregulation of 20 functional
216 pathways (Fig 2a and b, supplemental table 3). Key representative DEGs in these pathways are shown
217 in Fig. 3. Notably, we observed significant downregulation in pathways associated with
218 mitochondrial function (Fig. 2a). These included respiratory chain, synthesis and activity of NADH
219 dehydrogenase (quinone), and mitochondrial ribosome complex functions. Specifically, we identified
220 the downregulation of genes such as Atp5d, Cox5a, Mrpl14, Timm13, Tomm22, and Ndufa1, which
221 are crucial components of the mitochondrial electron transport chain, protein synthesis, and
222 mitochondrial transmembrane transport [45,46]. This downregulation suggests a reduction in
223 mitochondrial energy production and efficiency, which may contribute to lowered excitatory states in
224 PV-INs post-fluoxetine treatment [12]. Additionally, we observed downregulation in pathways
225 associated with ribosomes, including Rplp1, Rps13, and Rpl17 (Fig. 3b), which are involved in
226 ribosome biogenesis and function [47,48]. These reductions implicate decreased protein synthesis,
227 potentially affecting fundamental cellular functions and metabolism in PV-INs.

228

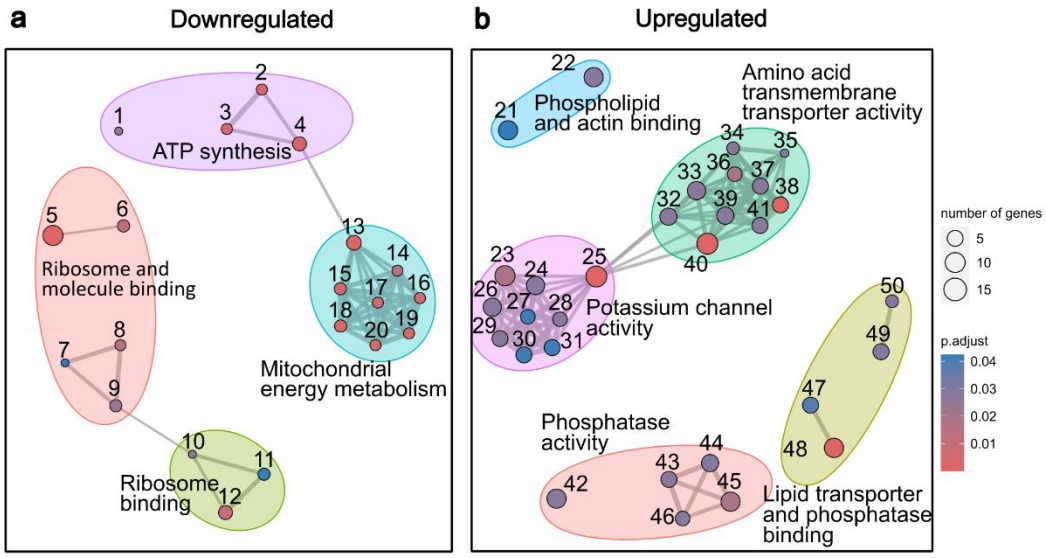

Figure 2: TRAP Analysis in PV-INs after Chronic Fluoxetine Treatment

a,b) Results of pathway enrichment analysis of GO Molecular Function -pathways in PV-INs clustered into 50 subgroups. Numbers correspond to individual pathways in Supplementary table 3. **a)** Downregulated pathways predominantly involve mitochondrial energy production, including NADH dehydrogenase activity, oxidoreductase activity, cytochrome c function, electron transport, proton transmembrane transport, and ATP synthase. Additionally, downregulation of ribosome-related pathways is observed, suggesting a broad impact on cellular metabolism and protein synthesis. **b)** Upregulated pathways are related to phosphatase activity, amino acid transmembrane transport, and voltage-gated potassium channels, highlighting enhanced synaptic and signaling activities [12]. The complete details of the 50 pathways are listed in supplemental table 3.

The upregulated pathways include those related to actin binding, phosphatase activity, amino acid transmembrane transport, voltage gated potassium channel activity, and ion gated channel activity (Fig. 2b). For instance, upregulated Wnk2 and Ptpn9 (Fig. 3c), which are associated with ion transport and cellular signaling pathways [49,50], suggests enhanced cellular communication, potentially contributing to altered intracellular signaling in PV-INs. Actin-binding proteins, which play a crucial role in dendritic spine formation and synaptic plasticity, were upregulated; this is consistent with previous findings that have established their role in structural

plasticity in neurons [51]. The increased phosphatase activity, particularly involving protein dephosphorylation, may indicate modulation of synaptic plasticity and signal transduction [52]. Furthermore, the upregulation of amino acid transport genes suggests enhanced neurotransmitter availability, which might support increased synaptic transmission and improved neuronal communication [53]. We also observed upregulation of Kcnf1, a voltage-gated potassium channel Kv5.1, which is involved in modulating the excitatory properties of PV-INs by acting as accessory subunit for other potassium channels [54].

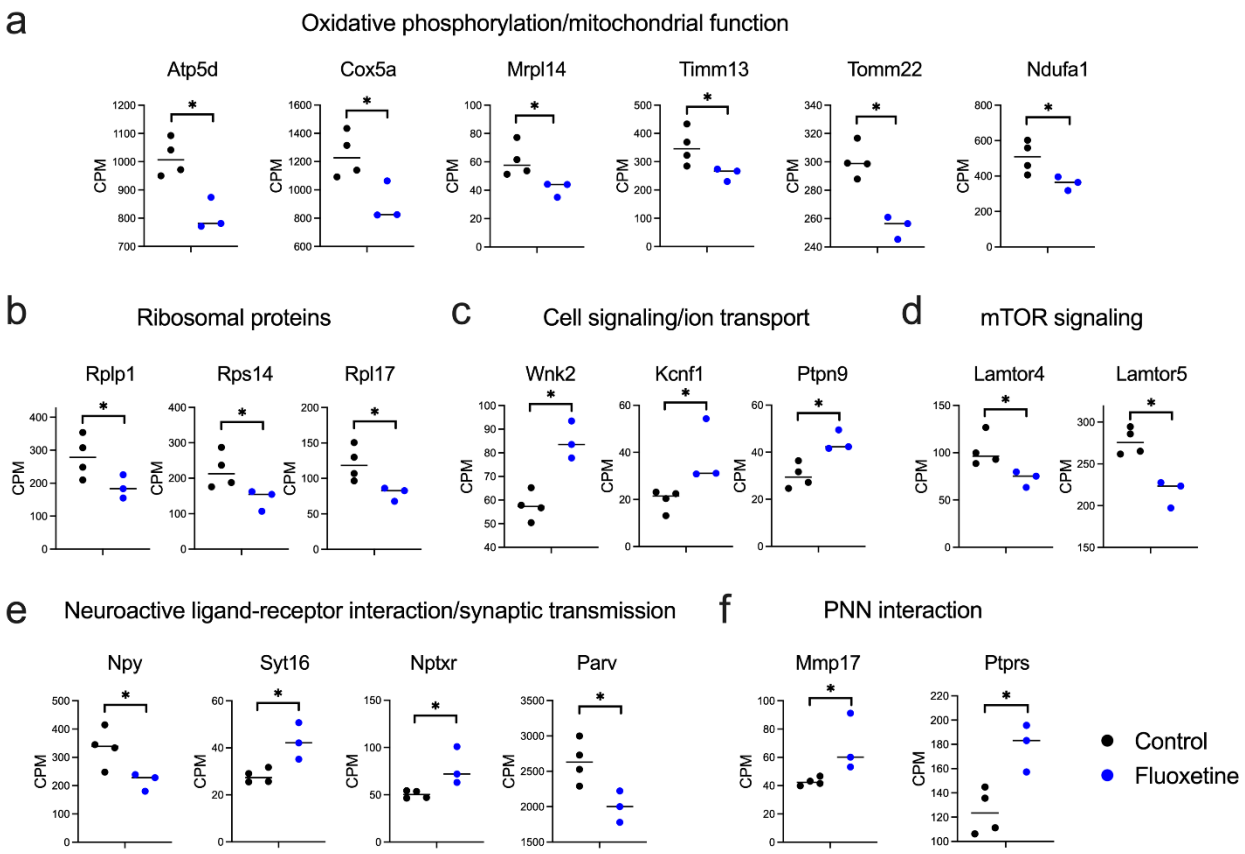

Figure 3: Representative DEGs After Chronic Fluoxetine Treatment

a) Oxidative Phosphorylation and Mitochondrial Function: Downregulated genes Atp5d, Cox5a, Mrpl14, Timm13, Tomm22, and Ndufa1 are critical components of the mitochondrial electron transport chain, protein synthesis and transmembrane transport. **b)** Ribosomal Proteins: Downregulated genes Rplp1, Rps13, and Rpl17 are involved in ribosome biogenesis and function,

indicating a potential decrease in protein synthesis capacity. **c)** Cell Signaling/Ion Transport: Upregulated genes Wnk2, Kcnf1, and Ptpn9 are associated with ion transport and signaling pathways. **d)** mTOR Signaling and Lysosomal Function: Downregulated genes Lamtor4 and Lamtor5 are part of the mTOR signaling pathway and lysosomal function. **e)** Neuroactive Ligand-Receptor Interaction/Synaptic Transmission: Downregulated genes Npy and Parv suggest reduced inhibitory signaling and calcium buffering. Upregulated genes Syt16 and Nptxr indicate enhanced synaptic transmission and receptor clustering. **f)** PNN interaction: Mmp17, an upregulated gene, plays a key role in matrix remodeling and may lead to the degradation of perineuronal nets (PNNs). Receptor type protein tyrosine phosphatase (Ptprs) was upregulated. It modulates TrkB activity in interaction with PNNs. * indicates statistical significance with $q < 0.1$.

In other pathways, downregulation of Lamtor4 and Lamtor5 within mTOR signaling and lysosomal function pathways (Fig. 3d) suggests suppression of cellular growth and metabolism, potentially reducing anabolic processes in PV-INs [55]. Additionally, downregulation of Neuropeptide Y (Npy) and Parvalbumin (Parv) (Fig. 3e) suggests weakened neuroactive ligand-receptor interaction and synaptic transmission. NPY enhances inhibitory tone and regulates stress and anxiety [56], while Parv, crucial for calcium buffering in fast-spiking interneurons, regulates neuronal excitability [57,58] and plasticity [11,12]. This may reduce inhibitory tone and disrupt calcium homeostasis in PV-INs. In contrast, the upregulation of Synaptotagmin 16 (Syt16) and Neuronal Pentraxin Receptor (Nptxr) suggests enhanced synaptic transmission and receptor clustering. Syt16, a member of the synaptotagmin family involved in synaptic vesicle exocytosis, may play a role in synaptic function, with other synaptotagmins, such as Syt4, being implicated in BDNF release [59]. Nptxr, which regulates AMPA receptor clustering, promotes synaptic plasticity and receptor localization at synapses [60]. This upregulation may increase excitatory signaling onto PV-INs, potentially altering the E/I balance in a complex manner. Lastly, we found upregulated genes interacting with PNN (Fig. 3f), including Matrix metalloproteinase-17 (Mmp17) (Fig. 3f). MMPs degrade extracellular matrix structures, such as the PNN [61]; the upregulation of Mmp17 may facilitate structural reorganization in response to chronic fluoxetine treatment, potentially modulating the activity of PV-INs [13,18]. In

293 contrast, Receptor type protein tyrosine phosphatase sigma (Ptprs), which interacts with chondroitin
294 sulfate proteoglycans (CSPGs) in PNNs, was upregulated (Fig. 3f), indicating a possible expressional
295 change after the PNN remodeling. Ptprs is also known to be involved in memory retention [17].[62]
296 These findings suggest that chronic fluoxetine treatment leads to a complex reorganization
297 of gene expression in PV-INs, with upregulated synaptic and neurotransmitter-related functions,
298 while simultaneously leading to reduced mitochondrial activity. This dual impact highlights the
299 intricate balance between promoting plasticity and altering cellular energy dynamics in response to
300 fluoxetine.
301
302 ***Chronic Fluoxetine Treatment Reduces Mitochondrial Membrane Potential in PV-INs***
303 To further investigate the impact of chronic fluoxetine treatment on mitochondrial function, we
304 measured mitochondrial membrane potential, mitochondrial mass, and intracellular ATP contents in
305 FACS-sorted cells after chronic fluoxetine administration.
306 A key finding was a marked reduction in mitochondrial membrane potential in PV-INs across
307 all brain regions after fluoxetine treatment ($p < 0.0001$) (Fig. 4a). In contrast, an increase in
308 membrane potential was observed specifically in non-PV cells of the PFC ($p < 0.0001$) (Fig. 4d). A
309 decrease in membrane potential typically indicates a reduction in ATP production by the
310 mitochondrial electron transport chain. Mitochondrial mass in PV-INs remained elevated in the PFC
311 with no significant changes in other brain regions post-treatment (Fig. 4b). Mitochondrial mass was,
312 however, reduced in non-PV cells after fluoxetine treatment ($p = 0.0071$) (Fig. 4e). Despite the
313 reduced membrane potential, no significant changes in ATP levels were detected in any cell type,
314 including PV-INs (Fig. 4c, f). Notably, ATP levels were higher in the PFC compared to the hippocampus
315 and other cortical regions, specifically in PV-INs ($p < 0.0001$), but fluoxetine treatment did not
316 significantly affect ATP levels (Fig. 4c).
317 These results suggest that while mitochondrial energy production remains active in PFC,
318 chronic fluoxetine treatment reduces energy production in PV-INs without alternating intracellular

319 ATP levels or mitochondrial mass. This reduction in PV-INs may contribute to the disinhibition of
320 other cortical cell types, particularly excitatory neurons, which could be reflected in the upregulation
321 of their energy production in non-PV-INs.
322
323

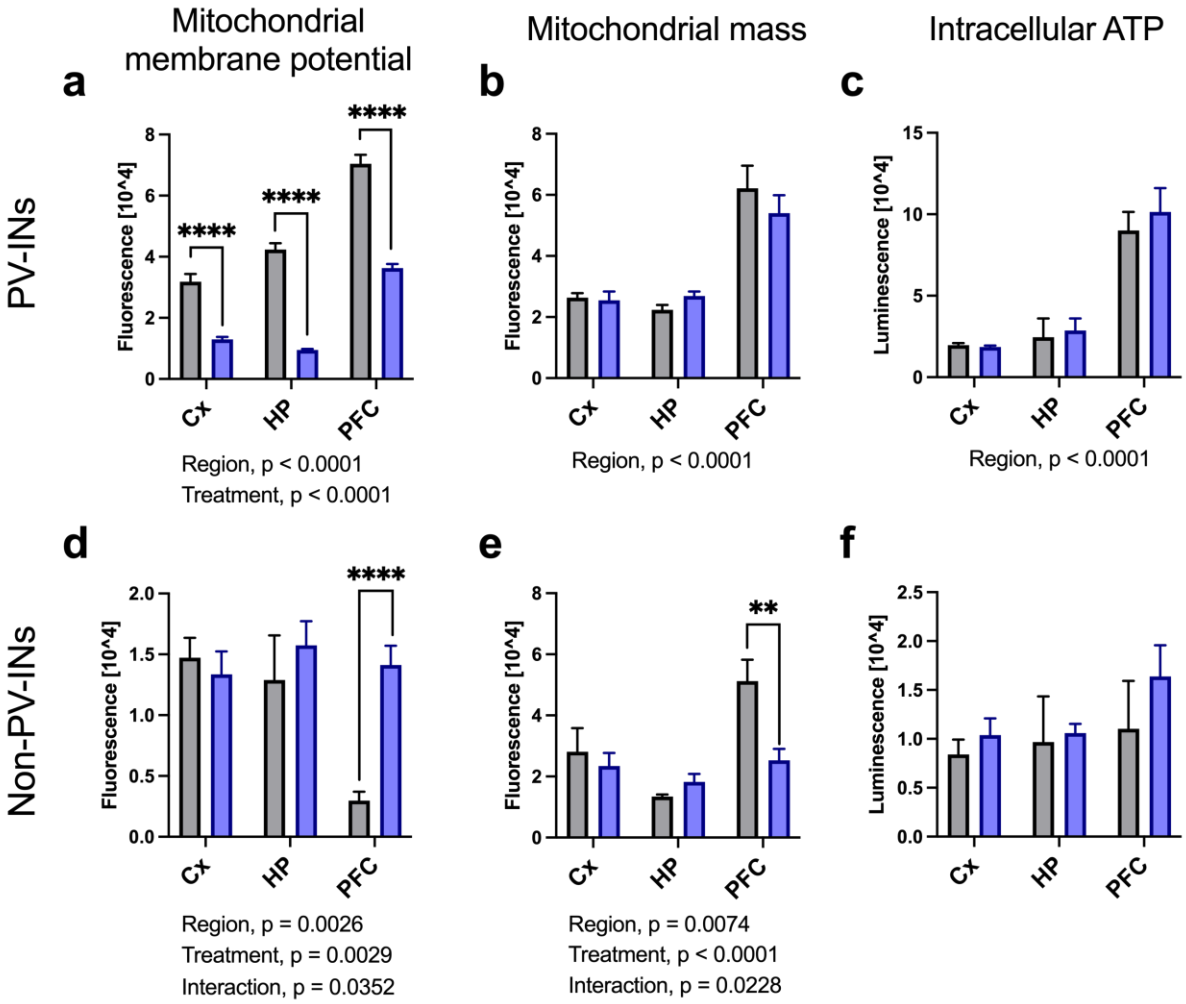

324

325 Figure 4: ATP production and mitochondria assays using FACS-sorted PV-INs and non-PV cells across
326 brain regions.

327 PV and other types of cells were sorted and analyzed separately in the cortex (Cx),
328 Hippocampus (HP), and prefrontal cortex (PFC): PV-INs, a, b, c; Non-PV-Cells, d, e, f. **(a)**
329 Mitochondrial membrane potential was significantly downregulated in PV-INs from all
330 studied regions following chronic fluoxetine treatment (Two-way ANOVA, Treatment, F (1,
331 95348) = 325.4, P < 0.0001). Regional differences were also observed (Two-way ANOVA,
332 region, F (2, 95348) = 160.2, P < 0,0001). (d) In contrast, upregulation of mitochondrial

membrane potential was shown in non-PV-INs from only the PFC (Two-way ANOVA , Treatment, F (1, 18669) = 4.438, P=0.0352; Šídák's multiple comparisons test ”control” vs ”fluoxetine”, PFC: P < 0.0001). **(b,e)** No differences in mitochondrial mass were seen in PV-cells, while it was down-regulated in non-PV-cells from the PFC (Two-way ANOVA, Treatment, F (1, 3617) = 5.191, P=0.0228; Šídák's multiple comparisons test, PFC: P = 0.0071). Regional differences were also observed both in PV-INs (Two-way ANOVA, Region: F(2, 32755) = 64.57, P < 0.0001) and non-PV-INs (Two-way ANOVA, Region: F(2, 3617) = 11.17, P < 0.0001). **(c,f)** No differences in intracellular ATP were seen after fluoxetine treatment in either cell type, while regional differences in ATP levels were detected in PV-INs (Two-way ANOVA, Region, F (2, 12) = 120.6, P<0.0001). Bars represent standard error of means, with ANOVA results noted below each plot. **, p < 0.01; ****, p < 0.0001.

Chronic Fluoxetine Modulates PV Cell distribution and PNN Structure in the PFC

To investigate plastic changes and mitochondrial distribution in specific subregions of the prefrontal cortex (PFC), we performed immunohistochemical analysis staining with antibodies of PV and PNN, plastic markers of PV-INs, and TOMM22, a marker of mitochondrial mass and function (Fig 5a). The analysis was focused on the prelimbic area (PL), infralimbic area (IL), and anterior cingulate area with supplementary motor area (ACA/M2), based on a reference atlas [42]. There was no treatment effect of fluoxetine on number of PV-INs or the proportion of PV-INs surrounded by PNNs (Fig. 5b, c). However, significant sub-regional differences in both the number of PV-INs and the ratio of PNN-positive PV-INs were observed across the subregions (Fig. 5b, c).

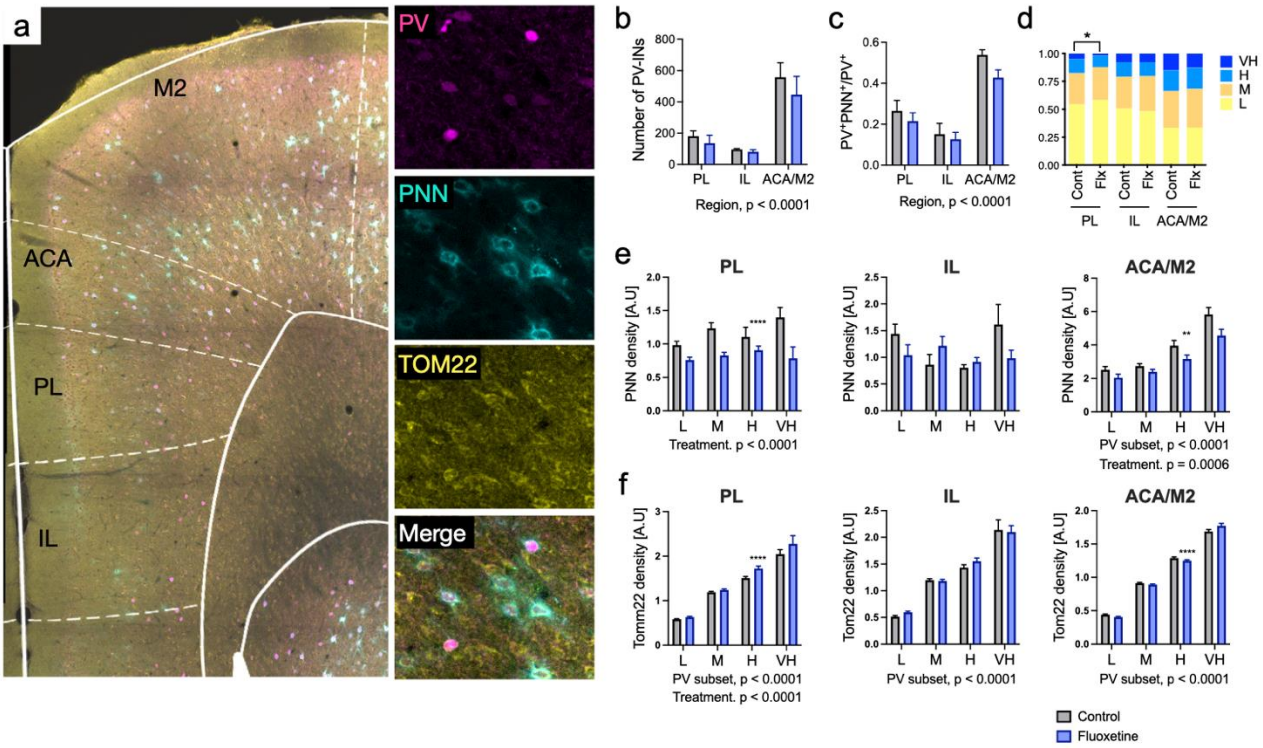

Figure 5: Immunostaining and imaging analysis PV, PNN and TOMM22in the PFC.

a) Immunostaining and imaging analysis were performed to assess parvalbumin (PV), perineuronal nets (PNN), and TOMM22, a quantitative mitochondrial marker. Sub-regions of the prefrontal cortex, including the infralimbic region (IL), prelimbic region (PL), and anterior cingulate area with secondary motor cortex (ACA/M2), were identified using a reference atlas and selected for subsequent analysis. **b)** Number of PV-INs in different subregions. Fluoxetine treatment did not have a significant effect on cell count. However, significant regional differences are observed ($F(2, 18) = 22.53$, $p < 0.0001$). **c)** The proportion of PV-positive cells surrounded by PNN. Although no significant treatment effect was observed, the ratio of PNN-positive PV cells varied significantly among regions (two-way ANOVA, Region, $F(2, 18) = 36.35$, $p < 0.0001$). **d)** PV-positive cells were categorized into four subgroups based on PV expression levels. The relative number of cells expressing very high levels of PV was significantly lower in the PL region following fluoxetine treatment (Chi-square test, $p = 0.0175$). **e)** The intensity of PNNs in PV-cell subsets (low, middle, high, and very high PV expression) was analyzed after chronic fluoxetine treatment in the PL, IL, and ACA/M2 regions. In both the PL and ACA/M2 regions, fluoxetine treatment significantly reduced the overall intensity of PNNs (Two-way ANOVA, Treatment, PL: $F(1, 335) = 17.28$, $p < 0.0001$; ACA/M2: Treatment, $F(1, 1744) = 11.68$, $p = 0.0006$). Additionally, there was a significant

374 effect of PV expression subsets (Two-way ANOVA, PV subset, ACA/M2: $F(3, 1744) = 40.64$, p
375 $= 0.0006$), indicating a positive correlation between PNN intensity and PV expression in the
376 ACA/M2 region. **f)** The intensity of TOMM22 in PV-cell subsets. In all regions, a significant
377 effect of PV expression subsets was observed (Two-way ANOVA, PV subset, PL: $F(3, 1287) =$
378 791.0 $p < 0.0001$; IL: $F(3, 714) = 390.7$, $p < 0.0001$; ACA/M2: $F(3, 4012) = 2756$, $p < 0.0001$),
379 indicating that PV-INs with higher PV expression exhibited higher TOMM22 levels compared
380 to those with lower PV expression. Fluoxetine treatment significantly increased TOMM22
381 expression only in the PL region (Two-way ANOVA, Treatment, $F(1, 1287) = 21.17$, $p <$
382 0.0001). Bars represent standard error of means, with ANOVA results noted below each plot.
383 **, $p < 0.01$; ****, $p < 0.0001$

384

385 PV-positive cells were categorized into four subgroups based on PV expression levels, as
386 previous studies have shown a negative correlation between PV expression intensity and plasticity in
387 PV-INs [6,11,12]. Chronic fluoxetine treatment led to a significant decrease in the number of cells
388 expressing very high levels of PV, particularly in the PL region ($p = 0.0175$) (Fig. 5d), which is
389 consistent with previous findings in the visual cortex [12] and hippocampus [6]. The analysis of PNNs
390 revealed a significant reduction in total PNN intensity in both the PL and ACA/M2 regions following
391 fluoxetine treatment (PL, $p < 0.0001$; ACA/M2, $p = 0.0006$). Additionally, there was a significant effect
392 of PV expression subsets, with a positive correlation between PNN intensity and PV expression levels
393 in the ACA/M2 region ($p = 0.0006$) (Fig. 5e). TOMM22 intensity across PV-IN subsets showed a
394 significant increase in TOMM22 expression only in the PL region post-treatment ($p < 0.0001$) (Fig.
395 5e). In all regions, PV-INs with higher PV expression exhibited higher TOMM22 levels than those with
396 lower PV expression ($p < 0.0001$).
397 These results suggest that chronic fluoxetine treatment induces notable changes in PV cell
398 plasticity and PNN structure, especially in the PL and ACA/M2 regions. The reduction in the number
399 of high PV-expressing PV-INs and corresponding PNN intensity implies increased plasticity in these
400 regions. Although no overall TOMM22 loss was detected following fluoxetine treatment, as observed

401 in the TRAP analysis, the correlation between TOMM22 and PV expression suggests that high PV-
402 expressing PV-INs may have a high energy consumption.
403
404 **Discussion**
405 Here we demonstrated that chronic fluoxetine treatment in mice induced transcriptional changes in
406 PV-INs, notably downregulating mitochondrial energy production, as reflected by the reduced
407 mitochondrial membrane potential in PV-INs of the PFC. In contrast, non-PV-INs exhibited an
408 increase in membrane potential. Despite mitochondrial mass and ATP levels remained stable, these
409 observations suggest that fluoxetine may exert opposing effects on mitochondrial efficiency between
410 PV-INs and other cells in the PFC. Altered genetic pathways related to voltage-gated potassium
411 channels, phosphatase activity, phospholipid binding, and extracellular matrix remodeling indicate
412 broader impacts on cellular communication and metabolism. Immunohistochemical analysis
413 corroborated these findings, revealing reductions in PV expression and perineuronal nets (PNNs)
414 without significant changes in TOMM22 intensity, highlighting consistent mitochondrial mass. These
415 results underscore the complexity of fluoxetine's effects on PV-INs, particularly in energy metabolism
416 and synaptic plasticity.
417
418 *Role of TrkB Activation and Synaptic Plasticity*
419 Chronic fluoxetine treatment has been found to enhance TrkB activation [8], the receptor for brain-
420 derived neurotrophic factor (BDNF), which plays a pivotal role in synaptic plasticity, neuronal survival,
421 and growth [8,62], especially in PV-INs [6,12]. Our TRAP analysis identified notable upregulation of
422 pathways associated with synaptic plasticity, including actin binding, voltage-gated potassium
423 channel activity, and amino acid transmembrane transport. In addition, we further observed
424 downregulation of Parvalbumin, and genes related to and perineuronal nets (PNNs). Previous studies
425 have demonstrated that chronic fluoxetine treatment or activation of TrkB in PV-INs reduces PNN
426 formation [5,6,12,63,64]. Additionally, enzymatic removal of the PNN has been shown to enhance

427 synaptic remodeling and restore juvenile-like plasticity, which is dependent on TrkB expression in PV-
428 INs [65]. These findings suggest that fluoxetine promotes a state of enhanced plasticity via TrkB
429 activation in PV-INs.
430
431 *Mitochondrial Dynamics, potassium channel regulation, and Impact on E/I Balance*
432 We observed both a reduction in mitochondrial membrane potential in PV-INs and an increase in
433 non-PV-INs. Since mitochondrial membrane potential is generated by electron transport chain
434 complexes I-IV and is used to produce ATP by complex V, ATP synthase [22], our findings demonstrate
435 that energy metabolism is decreased in PV-INs and increased in non-PV-INs. This shift may contribute
436 to a disinhibition of excitatory neurons, which compose a large part of the non-PV-INs. PV-INs are
437 crucial for maintaining the E/I balance in cortical circuits, with dysregulation linked to psychiatric
438 conditions such as depression [66,67]. Despite widespread transcriptional changes and
439 downregulation of mitochondrial membrane potential, we did not observe fluoxetine effects on
440 intracellular ATP levels; possibly due to the broad cellular functions ATP supports, maintaining
441 constant concentration even as its production altered. Additionally, technical limitations such as the
442 sensitivity of ATP detection assays and the rapid, localized turnover of ATP might have masked subtle
443 changes. The heterogeneity of cell populations in PV-INs could further dilute small ATP changes, and
444 the dynamic nature of ATP production may require more sensitive, real-time measurements.
445 Our previous study demonstrated that optical activation of TrkB specifically in PV-INs reduces their
446 excitability via the decreased expression and activity of Kv3.1 [12]. The activation of TrkB via BDNF
447 stimulation similarly modulate excitability and immune responses in the rat olfactory bulb [68].
448 Conversely, upregulation of Kv3.1b/3.2 channels in response to TrkB ligands BDNF and NT4 has been
449 observed in cultured rat neurons from the visual cortex [69]. These channels are crucial for fast
450 repolarization following an action potential, particularly in fast-spiking interneurons like PV-INs [70].
451 The differential regulations of the potassium channels observed across these studies likely reflect

452 their complexity, with region- specific roles and developmental, as well as activity-dependent,
453 variations in their expression [71].
454 Together, combination of the increased potassium channel gene expression, downregulation of
455 parvalbumin and PNNs, and reduced energy dynamics following fluoxetine treatment suggests a
456 reduction in the inhibitory tone of PV-INs. This shift potentially contributes to the E/I balance
457 alterations towards increased excitation and promoting synaptic plasticity and the remodeling of
458 cortical circuits, which are essential for cognitive flexibility and emotional regulation [15].
459
460 *Region-specific modulation of PV-IN plasticity in the prefrontal cortex by chronic fluoxetine treatment*
461 Our study reveals region-specific effects of chronic fluoxetine treatment on PV-INs across key
462 subregions of PFC, aligning with their distinct roles in emotional and cognitive processing. In the PL,
463 associated with fear expression, fluoxetine reduced PV expression, suggesting enhanced plasticity
464 that may aid in emotional regulation and anxiety relief [33,34]. While no significant changes were
465 observed in the IL, critical for fear extinction, the trend toward reduced inhibitory tone could support
466 the formation of new, less fearful associations [72]. In the ACA/M2, which are involved in cognitive
467 flexibility and motor planning, reduced perineuronal net (PNN) intensity points to increased synaptic
468 remodeling, potentially enhancing adaptability and cognitive function [35]. These findings highlight
469 that fluoxetine's region-specific enhancement of plasticity in the PFC contribute to its therapeutic
470 effects in treating depression and anxiety by modulating neural circuits related to emotion and
471 cognition.
472
473 *Clinical Implications and Future Directions*
474 The modulation of PV-INs by fluoxetine carries significant clinical implications, particularly given their
475 crucial role in maintaining cortical network balance. Fluoxetine's ability to reduce PV expression and
476 PNN density may help restore E/I balance in conditions with pathologically elevated inhibition,
477 offering therapeutic benefits in mood disorders and other neuropsychiatric conditions characterized

478 by disrupted cortical networks [9]. Our findings highlight potential biomarkers related to PV-IN
479 plasticity or mitochondrial activity, which could aid in identifying new therapeutic targets. Future
480 research should focus on exploring the long-term effects of fluoxetine on neural circuitry and
481 cognitive function to better understand its full spectrum of therapeutic outcomes. Additionally,
482 translational research should investigate combining fluoxetine with psychotherapy [2] or treatments
483 targeting complementary pathways, such as synaptic stabilization [73], to enhance its efficacy and
484 broaden its applicability in treating various neuropsychiatric disorders.
485

486 Acknowledgments
487 The authors would like to thank Sulo Kolehmainen and Seija Lågas for technical help. We also thank
488 the Biomedicum Flow cytometry unit at the University of Helsinki for instructing Sony SH800Z Cell
489 Sorter. We thank Biomedicum Imaging unit at the University of Helsinki for providing equipment and
490 technical help for immunohistochemical analysis. This work was carried out with the support of
491 HiLIFE Laboratory Animal Center Core Facility, the University of Helsinki, Finland. Next generation
492 sequencing was performed at the Institute for Molecular Medicine Finland FIMM Genomics unit
493 supported by HiLIFE and Biocenter Finland. The authors thank Emmy Lyytikäinen for language
494 revision.
495

496 Funding
497 These studies have been supported by grants by the Academy of Finland (294710, 303124, 307416,
498 327192), Sigrid Jusélius Foundation, Jane & Aatos Erkko Foundation, the Helsinki Institute of Life
499 Science (HiLIFE) Fellow Program, Bilateral exchange program between the Academy of Finland and
500 JSPS (Japan Society for the Promotion of Science), The Finnish Medical Foundation, and Biomedicum
501 Helsinki Foundation.
502

503 Conflict of Interest

EC is a co-founder and Board member of Kasvu Therapeutics. The other authors declare no competing financial interests.

Author Contributions

JU and EC conceived of and designed the project. EJ conducted all experiments including TRAP analysis, immunohistochemistry, imaging, and mitochondrial analysis under the supervision of JU. IS conducted imaging analysis. All authors were involved in writing the manuscript.

513

514 **References**

515 1. Castrén E, Hen R. Neuronal plasticity and antidepressant actions. Trends Neurosci.
516 2013;36:259–267.

517 2. Umemori J, Winkel F, Didio G, Llach Pou M, Castrén E. iPlasticity: Induced juvenile-like
518 plasticity in the adult brain as a mechanism of antidepressants. Psychiatry Clin Neurosci.
519 2018;72:633–653.

520 3. Castrén E. Is mood chemistry? Nat Rev Neurosci. 2005;6:241–246.

521 4. Vetencourt JFM, Sale A, Viegi A, Baroncelli L, De Pasquale R, O'Leary OF, et al. The
522 antidepressant fluoxetine restores plasticity in the adult visual cortex. Science (1979).
523 2008;320:385–388.

524 5. Karpova NN, Pickenhagen A, Lindholm J, Tiraboschi E, Kulesskaya N, Ágústsdóttir A, et al. Fear
525 Erasure in Mice Requires Synergy Between Antidepressant Drugs and Extinction Training.
526 Science (1979). 2011;334:1731–1734.

527 6. Jetsonen E, Didio G, Winkel F, Llach Pou M, Boj C, Kuczynski-Noyau L, et al. Activation of TrkB
528 in Parvalbumin interneurons is required for the promotion of reversal learning in spatial and
529 fear memory by antidepressants. Neuropsychopharmacology. 2023. March 21, 2023.
530 https://doi.org/10.1038/S41386-023-01562-Y.

531 7. Malberg JE, Duman RS. Cell Proliferation in Adult Hippocampus is Decreased by Inescapable
532 Stress: Reversal by Fluoxetine Treatment. Neuropsychopharmacology. 2003;28:1562–1571.

533 8. Casarotto PC, Girych M, Fred SM, Kovaleva V, Moliner R, Enkavi G, et al. Antidepressant drugs
534 act by directly binding to TRKB neurotrophin receptors. Cell. 2021;184:1299-1313.e19.

535 9. Sohal VS, Zhang F, Yizhar O, Deisseroth K. Parvalbumin neurons and gamma rhythms enhance
536 cortical circuit performance. Nature. 2009;459:698–702.

537 10. Bartos M, Vida I, Jonas P. Synaptic mechanisms of synchronized gamma oscillations in
538 inhibitory interneuron networks. Nat Rev Neurosci. 2007;8:45–56.

539 11. Donato F, Rompani SB, Caroni P. Parvalbumin-expressing basket-cell network plasticity
540 induced by experience regulates adult learning. Nature. 2013;504:272–276.

541 12. Winkel F, Ryazantseva M, Voigt MB, Didio G, Lilja A, Llach Pou M, et al. Pharmacological and
542 optical activation of TrkB in Parvalbumin interneurons regulate intrinsic states to orchestrate
543 cortical plasticity. Mol Psychiatry. 2021;26:7247–7256.

544 13. Fawcett JW, Oohashi T, Pizzorusso T. The roles of perineuronal nets and the perinodal
545 extracellular matrix in neuronal function. Nat Rev Neurosci. 2019;20:451–465.

546 14. Kwok JCF, Dick G, Wang D, Fawcett JW. Extracellular matrix and perineuronal nets in CNS
547 repair. Dev Neurobiol. 2011;71:1073–1089.

548 15. Ferguson BR, Gao W-J. PV Interneurons: Critical Regulators of E/I Balance for Prefrontal
549 Cortex-Dependent Behavior and Psychiatric Disorders. Front Neural Circuits. 2018;12.

550 16. Frischknecht R, Heine M, Perrais D, Seidenbecher CI, Choquet D, Gundelfinger ED. Brain
551 extracellular matrix affects AMPA receptor lateral mobility and short-term synaptic plasticity.
552 Nat Neurosci. 2009;12:897–904.

553 17. Lesnikova A, Casarotto P, Moliner R, Fred SM, Biojone C, Castrén E. Perineuronal Net Receptor
554 PTPσ Regulates Retention of Memories. Front Synaptic Neurosci. 2021;13.

555 18. Tewari BP, Chaunsali L, Campbell SL, Patel DC, Goode AE, Sontheimer H. Perineuronal nets
556 decrease membrane capacitance of peritumoral fast spiking interneurons in a model of
557 epilepsy. Nat Commun. 2018;9:4724.

558 19. Alaiyed S, McCann M, Mahajan G, Rajkowska G, Stockmeier CA, Kellar KJ, et al. Venlafaxine
559 Stimulates an MMP-9-Dependent Increase in Excitatory/Inhibitory Balance in a Stress Model
560 of Depression. The Journal of Neuroscience. 2020;40:4418–4431.

561 20. Cheng A, Hou Y, Mattson MP. Mitochondria and neuroplasticity. ASN Neuro. 2010;2:243–256.

562 21. Mattson MP. Mitochondrial regulation of neuronal plasticity. Neurochem Res. 2007;32:707–
563 715.

564 22. Wong-Riley MTT. Cytochrome oxidase: an endogenous metabolic marker for neuronal activity.
565 Trends Neurosci. 1989;12:94–101.

566 23. Yano M, Terada K, Mori M. Mitochondrial Import Receptors Tom20 and Tom22 Have
567 Chaperone-like Activity. Journal of Biological Chemistry. 2004;279:10808–10813.

568 24. Kravic B, Harbauer AB, Romanello V, Simeone L, Vögtle F-N, Kaiser T, et al. In mammalian
569 skeletal muscle, phosphorylation of TOMM22 by protein kinase CSNK2/CK2 controls
570 mitophagy. Autophagy. 2018;14:311–335.

571 25. de Oliveira MR. Fluoxetine and the mitochondria: A review of the toxicological aspects. Toxicol
572 Lett. 2016;258:185–191.

573 26. Filipović D, Costina V, Perić I, Stanisavljević A, Findeisen P. Chronic fluoxetine treatment directs
574 energy metabolism towards the citric acid cycle and oxidative phosphorylation in rat
575 hippocampal nonsynaptic mitochondria. Brain Res. 2017;1659:41–54.

576 27. Curti C, Mingattao FE, Polizello ACM, Galastri LO, Uyemura SA, Santos AC. Fluoxetine interacts
577 with the lipid bilayer of the inner membrane in isolated rat brain mitochondria, inhibiting
578 electron transport and F1F0-ATPase activity. Mol Cell Biochem. 1999;199:103–109.

579 28. Hroudová J, Fišar Z. In vitro inhibition of mitochondrial respiratory rate by antidepressants.
580 Toxicol Lett. 2012;213:345–352.

581 29. Agostinho FR, Réus GZ, Stringari RB, Ribeiro KF, Ferreira GK, Jeremias IC, et al. Olanzapine plus
582 fluoxetine treatment alters mitochondrial respiratory chain activity in the rat brain. Acta
583 Neuropsychiatr. 2011;23:282–291.

584 30. Miller EK, Cohen JD. An Integrative Theory of Prefrontal Cortex Function. Annu Rev Neurosci.
585 2001;24:167–202.

586 31. Grace AA, Floresco SB, Goto Y, Lodge DJ. Regulation of firing of dopaminergic neurons and
587 control of goal-directed behaviors. Trends Neurosci. 2007;30:220–227.

588 32. Guirado R, Perez-Rando M, Ferragud A, Gutierrez-Castellanos N, Umemori J, Carceller H, et al.
589 A Critical Period for Prefrontal Network Configurations Underlying Psychiatric Disorders and
590 Addiction. Front Behav Neurosci. 2020;14.

591 33. Sotres-Bayon F, Cain CK, LeDoux JE. Brain Mechanisms of Fear Extinction: Historical
592 Perspectives on the Contribution of Prefrontal Cortex. Biol Psychiatry. 2006;60:329–336.

593 34. Quirk GJ, Mueller D. Neural Mechanisms of Extinction Learning and Retrieval.
594 Neuropsychopharmacology. 2008;33:56–72.

595 35. Bush G, Luu P, Posner MI. Cognitive and emotional influences in anterior cingulate cortex.
596 Trends Cogn Sci. 2000;4:215–222.

597 36. Hippenmeyer S, Vrieseling E, Sigrist M, Portmann T, Laengle C, Ladle DR, et al. A
598 Developmental Switch in the Response of DRG Neurons to ETS Transcription Factor Signaling.
599 PLoS Biol. 2005;3:e159.

600 37. Liu J, Krautzberger AM, Sui SH, Hofmann OM, Chen Y, Baetscher M, et al. Cell-specific
601 translational profiling in acute kidney injury. Journal of Clinical Investigation. 2014;124:1242–
602 1254.

603 38. Madisen L, Zwingman TA, Sunkin SM, Oh SW, Zariwala HA, Gu H, et al. A robust and high-
604 throughput Cre reporting and characterization system for the whole mouse brain. Nat
605 Neurosci. 2010;13:133–140.

606 39. Heiman M, Kulicke R, Fenster RJ, Greengard P, Heintz N. Cell type-specific mRNA purification
607 by translating ribosome affinity purification (TRAP). Nat Protoc. 2014;9:1282–1291.

608 40. Ting JT, Daigle TL, Chen Q, Feng G. Acute Brain Slice Methods for Adult and Aging Animals:
609 Application of Targeted Patch Clamp Analysis and Optogenetics2014. p. 221–242.

610 41. Emaus RK, Grunwald R, Lemasters JJ. Rhodamine 123 as a probe of transmembrane potential
611 in isolated rat-liver mitochondria: spectral and metabolic properties. Biochim Biophys Acta.
612 1986;850:436–448.

613 42. George Paxinos, Keith B. J. Franklin. The mouse brain in stereotaxic coordinates, 2nd edition.
614 Academic_Press; 2001.

615 43. Love MI, Huber W, Anders S. Moderated estimation of fold change and dispersion for RNA-seq
616 data with DESeq2. Genome Biol. 2014;15:1–21.

617 44. Wu T, Hu E, Xu S, Chen M, Guo P, Dai Z, et al. clusterProfiler 4.0: A universal enrichment tool
618 for interpreting omics data. The Innovation. 2021;2:100141.

619 45. den Brave F, Pfanner N, Becker T. Mitochondrial entry gate as regulatory hub. Biochimica et
620 Biophysica Acta (BBA) - Molecular Cell Research. 2024;1871:119529.

621 46. Sousa JS, D'Imprima E, Vonck J. Mitochondrial Respiratory Chain Complexes2018. p. 167–227.

622 47. Vanden Broeck A, Klinge S. Eukaryotic Ribosome Assembly. Annu Rev Biochem. 2024;93:189–
623 210.

624 48. Campos RK, Wijeratne HRS, Shah P, Garcia-Blanco MA, Bradrick SS. Ribosomal stalk proteins
625 RPLP1 and RPLP2 promote biogenesis of flaviviral and cellular multi-pass transmembrane
626 proteins. Nucleic Acids Res. 2020;48:9872–9885.

627 49. Tiganis T, Bennett AM. Protein tyrosine phosphatase function: the substrate perspective.
628 Biochemical Journal. 2007;402:1–15.

629 50. Rinehart J, Vázquez N, Kahle KT, Hodson CA, Ring AM, Gulcicek EE, et al. WNK2 Kinase Is a
630 Novel Regulator of Essential Neuronal Cation-Chloride Cotransporters. Journal of Biological
631 Chemistry. 2011;286:30171–30180.

632 51. Borovac J, Bosch M, Okamoto K. Regulation of actin dynamics during structural plasticity of
633 dendritic spines: Signaling messengers and actin-binding proteins. Molecular and Cellular
634 Neuroscience. 2018;91:122–130.

635 52. Shi Y. Serine/Threonine Phosphatases: Mechanism through Structure. Cell. 2009;139:468–
636 484.

637 53. Kanai Y, Hediger MA. The glutamate and neutral amino acid transporter family: physiological
638 and pharmacological implications. Eur J Pharmacol. 2003;479:237–247.

639 54. Kramer JW, Post MA, Brown AM, Kirsch GE. Modulation of potassium channel gating by
640 coexpression of Kv2.1 with regulatory Kv5.1 or Kv6.1 α-subunits. American Journal of
641 Physiology-Cell Physiology. 1998;274:C1501–C1510.

642 55. Bar-Peled L, Sabatini DM. Regulation of mTORC1 by amino acids. Trends Cell Biol.
643 2014;24:400–406.

644 56. Tasan RO, Verma D, Herzog H, Sperk G. Neuropeptide Y in the basolateral amygdala
645 modulates the acquisition of conditioned fear. BMC Pharmacol. 2010;10:A33.

646 57. Caillard O, Moreno H, Schwaller B, Llano I, Celio MR, Marty A. Role of the calcium-binding
647 protein parvalbumin in short-term synaptic plasticity. Proceedings of the National Academy of
648 Sciences. 2000;97:13372–13377.

649 58. Schwaller B. The continuing disappearance of “pure” Ca2+ buffers. Cellular and Molecular Life
650 Sciences. 2009;66:275–300.

651 59. Dean C, Liu H, Staudt T, Stahlberg MA, Vingill S, Bückers J, et al. Distinct Subsets of Syt-
652 IV/BDNF Vesicles Are Sorted to Axons versus Dendrites and Recruited to Synapses by Activity.
653 The Journal of Neuroscience. 2012;32:5398–5413.

654 60. Pelkey KA, Barksdale E, Craig MT, Yuan X, Sukumaran M, Vargish GA, et al. Pentraxins
655 Coordinate Excitatory Synapse Maturation and Circuit Integration of Parvalbumin
656 Interneurons. Neuron. 2015;85:1257–1272.

657 61. Alaiyed S, Conant K. A Role for Matrix Metalloproteases in Antidepressant Efficacy. Front Mol
658 Neurosci. 2019;12.

659 62. Minichiello L. TrkB signalling pathways in LTP and learning. Nat Rev Neurosci. 2009;10:850–
660 860.

661 63. Ohira K, Takeuchi R, Shoji H, Miyakawa T. Fluoxetine-Induced Cortical Adult Neurogenesis.
662 Neuropsychopharmacology. 2013;38:909–920.

663 64. Mikics É, Guirado R, Umemori J, Tóth M, Biró L, Miskolczi C, et al. Social Learning Requires
664 Plasticity Enhanced by Fluoxetine Through Prefrontal Bdnf-TrkB Signaling to Limit Aggression
665 Induced by Post-Weaning Social Isolation. Neuropsychopharmacology. 2018;43:235–245.

666 65. Lesnikova A, Casarotto PC, Fred SM, Voipio M, Winkel F, Steinzeig A, et al. Chondroitinase and
667 antidepressants promote plasticity by releasing TRKB from dephosphorylating control of ptpσ
668 in parvalbumin neurons. Journal of Neuroscience. 2021;41:972–980.

669 66. Sohal VS, Rubenstein JLR. Excitation-inhibition balance as a framework for investigating
670 mechanisms in neuropsychiatric disorders. Mol Psychiatry. 2019;24:1248–1257.

671 67. Marín O. Interneuron dysfunction in psychiatric disorders. Nat Rev Neurosci. 2012;13:107–
672 120.

673 68. Tucker K, Fadool DA. Neurotrophin modulation of voltage-gated potassium channels in rat
674 through TrkB receptors is time and sensory experience dependent. J Physiol. 2002;542:413–
675 429.

676 69. Grabert J, Wahle P. Neuronal activity and TrkB ligands influence Kv3.1b and Kv3.2 expression
677 in developing cortical interneurons. Neuroscience. 2008;156:618–629.

678 70. RUDY B, CHOW A, LAU D, AMARILLO Y, OZAITA A, SAGANICH M, et al. Contributions of Kv3
679 Channels to Neuronal Excitability. Ann N Y Acad Sci. 1999;868:304–343.

680 71. Johnston J, Forsythe ID, Kopp-Scheinpflug C. SYMPOSIUM REVIEW: Going native: voltage-
681 gated potassium channels controlling neuronal excitability. J Physiol. 2010;588:3187–3200.

682 72. Milad MR, Quirk GJ. Fear Extinction as a Model for Translational Neuroscience: Ten Years of
683 Progress. Annu Rev Psychol. 2012;63:129–151.

684 73. Duman RS, Sanacora G, Krystal JH. Altered Connectivity in Depression: GABA and Glutamate
685 Neurotransmitter Deficits and Reversal by Novel Treatments. Neuron. 2019;102:75–90.

686